Xylans Provide the Structural Driving Force for Mucilage Adhesion to the Arabidopsis Seed Coat[1]

Marie-Christine Ralet*, Marie-Jeanne Crépeau, Jacqueline Vigouroux, Joseph Tran, Adeline Berger, Christine Sallé, Fabienne Granier, Lucy Botran, and Helen M. North*

INRA, UR 1268 Biopolymères Interactions Assemblages, F–44316 Nantes, France (M.-C.R., M.-J.C., J.V.); and Institut Jean-Pierre Bourgin, Institut National de la Recherche Agronomique, AgroParisTech, CNRS, Université Paris-Saclay, RD10, 78026 Versailles cedex, France (J.T., A.B., C.S., F.G., L.B., H.M.N.)

ORCID IDs: 0000-0002-0292-5272 (M.-C.R.); 0000-0002-4624-0363 (J.T.); 0000-0001-6810-2853 (F.G.); 0000-0002-5749-2603 (H.M.N.).

Arabidopsis (*Arabidopsis thaliana*) seed coat epidermal cells produce large amounts of mucilage that is released upon imbibition. This mucilage is structured into two domains: an outer diffuse layer that can be easily removed by agitation and an inner layer that remains attached to the outer seed coat. Both layers are composed primarily of pectic rhamnogalacturonan I (RG-I), the inner layer also containing rays of cellulose that extend from the top of each columella. Perturbation in cellulosic ray formation has systematically been associated with a redistribution of pectic mucilage from the inner to the outer layer, in agreement with cellulose-pectin interactions, the nature of which remained unknown. Here, by analyzing the outer layer composition of a series of mutant alleles, a tight proportionality of xylose, galacturonic acid, and rhamnose was evidenced, except for *mucilage modified5-1* (*mum5-1*; a mutant showing a redistribution of mucilage pectin from the inner adherent layer to the outer soluble one), for which the rhamnose-xylose ratio was increased drastically. Biochemical and in vitro binding assay data demonstrated that xylan chains are attached to RG-I chains and mediate the adsorption of mucilage to cellulose microfibrils. *mum5-1* mucilage exhibited very weak adsorption to cellulose. *MUM5* was identified as a putative xylosyl transferase recently characterized as MUCI21. Together, these findings suggest that the binding affinity of xylose ramifications on RG-I to a cellulose scaffold is one of the factors involved in the formation of the adherent mucilage layer.

A characteristic of plant cells is the extracellular matrix of polysaccharides and proteins that form a rigid and resistant support while remaining malleable for growth and intercellular exchanges. The association of cellulose, hemicellulose, and pectin polymers provides both rigidity and plasticity thanks to their distinct structural properties and how they interact. The precise nature of these interactions remains an open question, with evidence for noncovalent binding of hemicellulose or rhamnogalacturonan I (RG-I) arabinan and galactan side chains to cellulose (Hayashi et al., 1987; Vincken et al., 1995; Zykwinska et al., 2005; Köhnke et al., 2011). Improving our knowledge of the interactions between cell wall polymers, therefore, is fundamental to our understanding of the regulation of plant growth and for their exploitation in biodegradable materials or biofuel production.

The polysaccharides produced by seed coat epidermal cells, notably those that form seed mucilage, are emerging as a powerful model system. In plant cell walls, polysaccharides are present as complex mixtures of polymers, often with essential functions, whereas the range of polysaccharides in a given seed mucilage are generally simpler in composition and their absence is not prejudicial. Mucilage polysaccharides are accumulated during seed development in the apoplasm of seed coat epidermal cells and released on imbibition of the mature, dry seed (Beeckman et al., 2000; Western et al., 2000; Windsor et al., 2000). In Arabidopsis (*Arabidopsis thaliana*), released mucilage appears as two distinct layers; the outer layer is soluble, whereas the inner layer is adherent and difficult to remove completely even with strong alkali solutions (Western et al., 2000, 2001; Macquet et al., 2007a). Both layers are composed mainly of unsubstituted RG-I and a pectic domain made of alternating (1,4)-α-D-GalA and (1,2)-α-L-Rha units (Ridley et al., 2001). In wild-type seeds, the outer layer can be recovered easily by gentle water, diluted ammonium oxalate, or diluted EDTA extraction at 20°C to 40°C (Usadel et al., 2004; Macquet et al., 2007a; Rautengarten et al., 2008; Arsovski et al., 2009). Rha and

[1] This work was supported by the National Research Agency program (grant no. ANR–08–BLAN–0061) and by Labex Saclay Plant Sciences-SPS (grant no. ANR–10–LABX–0040–SPS).

* Address correspondence to marie-christine.ralet@nantes.inra.fr and helen.north@versailles.inra.fr.

The author responsible for distribution of materials integral to the findings presented in this article in accordance with the policy described in the Instructions for Authors (www.plantphysiol.org) is: Helen M. North (helen.north@versailles.inra.fr).

M.-C.R. and H.M.N. conceived and supervised experiments; M.-J.C., J.V., A.B., C.S., J.T., L.B., M.-C.R., and H.M.N. performed experiments; M.-C.R., H.M.N., and F.G. analyzed the data; M.-C.R. and H.M.N. wrote and revised the article.

www.plantphysiol.org/cgi/doi/10.1104/pp.16.00211

GalA account for 90% to 95% of the sugars, with only traces of Ara, Xyl, Man, Gal, and Glc. The macromolecular characteristics of the outer layer RG-I indicates two populations, a major (more than 90%) homogenous one of approximately 600 kD and a minor one of very high molar mass corresponding to entangled, collapsed, or aggregated macromolecules (Macquet et al., 2007a). It has been hypothesized that the latter could originate from the inner layer (Macquet et al., 2007a).

Analysis of the polysaccharides in the inner layer of Arabidopsis mucilage is more complicated due to its resistance to extraction by aggressive chemical protocols (Macquet et al., 2007a). This can be overcome by digestion with pectolytic and cellulolytic enzymes in admixture after removal of the outer mucilage (Macquet et al., 2007a) or by high-speed mechanical agitation (Voiniciuc et al., 2015c). Coupled with in situ immunolabeling, these techniques have enabled detailed information to be obtained about the structure and composition of the inner layer. As well as RG-I, cellulose is present together with minor amounts of galactan, arabinan, mannan, and homogalacturonan (HG; Penfield et al., 2001; Willats et al., 2001; Macquet et al., 2007a; Arsovski et al., 2009; Harpaz-Saad et al., 2011; Sullivan et al., 2011; Saez-Aguayo et al., 2013; Yu et al., 2014; Voiniciuc et al., 2015c). The majority of the methylesterified HG labeled in adherent mucilage, however, has been shown to be derived from fragments of the outer cell wall trapped in the mucilage (Saez-Aguayo et al., 2013).

Mucilage is nonessential in laboratory conditions, simplifying the selection of mutants affected in mucilage production. Arabidopsis mutants with modified mucilage phenotypes have proved to be excellent tools for the identification of genes involved in the production of polysaccharides (for review, see North et al., 2014). A number of transcription factors have been identified that regulate seed coat differentiation and mucilage production. For example, mutants defective for the homeodomain transcription factor GLABRA2 (GL2) do not complete epidermal cell differentiation and show limited production of mucilage polysaccharides (Koornneef, 1981; Rerie et al., 1994; Western et al., 2001; Gonzalez et al., 2009). An exception is LEUNIG_HOMOLOG (LUH)/MUM1, which undergoes normal differentiation and appears to modulate mucilage release by controlling the expression of proteins involved in pectin maturation (Huang et al., 2011; Walker et al., 2011; Saez-Aguayo et al., 2013). The β-D-galactosidase MUM2 and bifunctional β-D-xylosidase/α-L-arabinofuranosidase BXL1 trim RG-I side chains, thereby modifying mucilage swelling and release (Dean et al., 2007; Macquet et al., 2007b; Arsovski et al., 2009), while the subtilisin-like Ser protease SBT1.7 and pectin methylesterase inhibitor PMEI6 modulate HG methylesterification of the outer primary cell wall of seed coat epidermal cells so that it fragments under the pressure of swelling mucilage polysaccharides (Rautengarten et al., 2008; Saez-Aguayo et al., 2013).

Mucilage mutants also have been identified that are affected in enzymes implicated in polysaccharide synthesis: *mucilage modified4* (*mum4*)/*rhamnose biosynthetic gene2* (*rhm2*), *galacturonosyltransferase-like5* (*gatl5*), and *galacturonosyltransferase11* (*gaut11*) have reductions in mucilage Rha and/or GalA contents (Usadel et al., 2004; Western et al., 2004; Oka et al., 2007; Caffall et al., 2009; Kong et al., 2013), whereas cellulose production is reduced in the inner mucilage layer of *cellulose synthase5* (*cesa5*)/*mum3*, the *cesa3* mutant *irregular xylem1-1* (*irx1-1*), and *fei2* (Harpaz-Saad et al., 2011; Mendu et al., 2011; Sullivan et al., 2011; Griffiths et al., 2015). Although the total amount of mucilage pectin is unchanged in the latter mutants, their partitioning is modified in *cesa5* and *fei2*, with a reduction observed in the inner layer demonstrating that cellulose plays a crucial role in anchoring mucilage pectin to the seed coat surface. Similarly, *salt overly sensitive5* (*sos5*), *irx14*, and *mum5* mutants exhibit a redistribution of pectin to the outer mucilage layer, suggesting altered polysaccharide interactions (Macquet et al., 2007a; Harpaz-Saad et al., 2011; Sullivan et al., 2011; Griffiths et al., 2014; Voiniciuc et al., 2015a). As *cesa5 sos5* mutants have more severely affected mucilage partitioning, it appears that the arabinogalactan protein SOS5 modulates pectin adherence independently from cellulose and that mucilage pectin is attached to the seed by at least two independent mechanisms (Griffiths et al., 2014). The identity and molecular role of MUM5 remained to be determined (North et al., 2014). Here, mapping combined with whole-genome resequencing were employed to identify MUM5, which is predicted to encode a putative xylosyl transferase recently characterized as MUCI21 by Voiniciuc et al. (2015a). Furthermore, a unique population of RG-I with xylan side branches was identified in wild-type mucilage that mediated the adsorption of mucilage to cellulose microfibrils in in vitro binding assays. The absence of these side branches in the mucilage of *mum5* mutants is in agreement with a role for MUM5 in the synthesis of the RG-I xylan side branches and demonstrates their crucial role in the formation of the adherent mucilage layer.

RESULTS

Xyl Contents in Outer Soluble Mucilage Show Tight Proportionality to Those of Rha and GalA

In a screen for mucilage-release mutants from the Versailles collection of transfer DNA (T-DNA) mutants, a series of mutant alleles were identified in previously known genes. These mutant alleles were all in the Wassilewskija (Ws) accession and provided the opportunity for a comparative study of their effect on mucilage production. Mucilage was extracted in a similar manner to that described previously for the *mum2* mucilage-release mutant (Macquet et al., 2007b), with HCl-NaOH extraction of nonattached and loosely attached mucilage (North et al., 2014) followed by rhamnogalacturonan hydrolase (RGase) digestion of the inner mucilage layer. The composition and total

sugar contents were then determined for both layers. The total amounts of mucilage sugars and their partitioning between the outer and inner layers in the different mutants compared with the wild type are shown in Figure 1 and Supplemental Table S1. In *gl2* mutant alleles, the total amount of sugars was reduced drastically compared with the wild type, in agreement with previous analyses (Western et al., 2001). Furthermore, a clear redistribution from the outer soluble layer to the inner adherent layer was observed. *luh* and *mum2* mutants also showed reduced levels of total sugars and modified partitioning from the outer soluble layer to the inner adherent layer, as reported previously for *mum2* (Dean et al., 2007; Macquet et al., 2007b). In contrast, in the *sbt1.7-3* mutant, neither mucilage sugar amounts nor partitioning appeared unaltered, in agreement with the hypothesis that SBT1.7 is required for correct fragmentation of the outer primary cell wall of seed coat epidermal cells (Rautengarten et al., 2008) and does not affect mucilage production itself.

Individual neutral and acidic sugar contents in each mucilage layer were examined by generating a correlation heat map (Fig. 2). The mutant chemotypes grouped with one cluster for the four *gl2* mutant alleles and a second for the *luh* and *mum2* mutants as expected; the *sbt1.7-3* mucilage composition was most similar to the wild type. In agreement with the major component of mucilage being RG-I, the most significant correlation between sugars in each layer was between Rha and GalA contents. Intriguingly, soluble mucilage Xyl contents clustered tightly with Rha and GalA contents (Fig. 2). In effect, a clear linear relationship was observed between Xyl and Rha contents between genotypes, with on average one Xyl unit for 16 Rha units (Fig. 3).

In order to gain further insight into the significance of this proportionality, mucilage from *mum5* and *cesa5* was examined, as they both have been shown to exhibit a redistribution of mucilage from the inner to the outer layer (Macquet et al., 2007a; Harpaz-Saad et al., 2011; Mendu et al., 2011; Sullivan et al., 2011). Mucilage was extracted as described for genotypes in the Ws accession followed by an additional extraction using Maxazyme, a cellulase-hemicellulase cocktail. *cesa5-2* and *mum5-1* both showed increases in Rha and GalA in the HCl-NaOH extract, with concomitant decreases in the same sugars in the RGase hydrolysate (Table I), confirming the redistribution of RG-I between the outer and adherent mucilage in *mum5* and *cesa5* mutants. *cesa5-2* also showed a clear decrease in Glc in the Maxazyme hydrolysate (Table I), confirming that *cesa5* contains less mucilage cellulose (Harpaz-Saad et al., 2011; Mendu et al., 2011; Sullivan et al., 2011). In contrast, Glc contents did not decrease in *mum5-1* mucilage extracts (Table I). Furthermore, when the proportions of Xyl and Rha were plotted, wild-type Columbia-0 (Col-0), wild-type Columbia-2 (Col-2), and *cesa5-2* fell perfectly onto the previously established linear fit, whereas *mum5-1* showed a reduction in the proportion of Xyl (Fig. 3). To confirm that the modified *mum5-1* Xyl contents were indeed due to differences in mucilage composition and did not result from contamination of outer mucilage extracts with polymers derived from cell walls of the outer seed coat released by HCl-NaOH treatment, a gentle water extraction of mucilage was carried out. The sugar contents of these extracts showed an even greater difference in the amounts of Rha and GalA to Xyl for *mum5-1* compared with wild-type Col-2, while the amounts of other minor sugars were unaffected (Supplemental Table S2). Consequently, the Rha-Xyl ratio was increased drastically in *mum5-1* water-extractable mucilage compared with wild-type Col-2 (Supplemental Table S2).

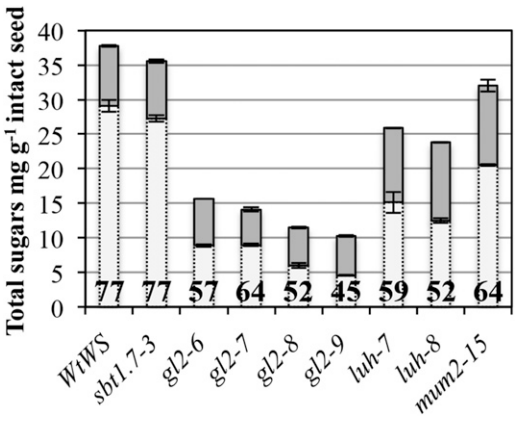

Figure 1. Seed mucilage amounts and partitioning are modified in *gl2*, *mum1*, and *mum2*. Total sugar amounts are shown for HCl-NaOH-extracted outer mucilage (light gray bars) and RGase-extracted inner mucilage (dark gray bars). Values are means of two biological repeats ± SD. The percentage of mucilage recovered in the HCl-NaOH-soluble fraction is indicated within the light gray bars.

Tailored Water-Soluble Mucilage from the Wild Type, But Not *mum5*, Adsorbs to Cellulose in Vitro

The tight proportionality of Xyl-GalA-Rha suggested that xylan side chains could be covalently linked to the RG-I backbone in Arabidopsis seed mucilage, as has been observed in polysaccharides from leaves of *Diospyros kaki* (Duan et al., 2004; Tan et al., 2013) and Arabidopsis suspension culture medium (Tan et al., 2013). Xylan backbones are very similar in structure to cellulose, with both macromolecules built of glycopyranose rings in the $^4C_1$ chair conformation linked to one another by β-1,4 diequatorial glycosidic bonds. This means that the gross features of their potential energy surfaces are very similar (Mazeau and Charlier, 2012). As such, there is a high affinity between the two species, and xylan adsorbs irreversibly onto cellulose surfaces (Kabel et al., 2007; Köhnke et al., 2011). Therefore, it is possible that xylan side chains could participate in anchoring mucilage pectin to the seed coat surface through noncovalent interactions with cellulose.

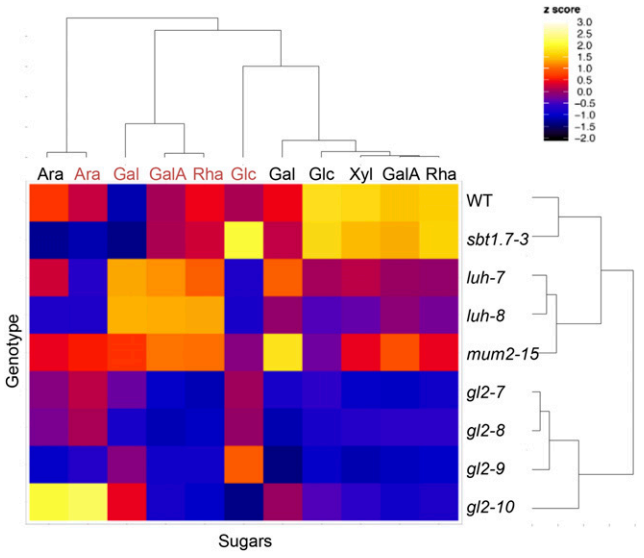

Figure 2. Clustering of sugars based on their quantity in outer or inner mucilage layers of Arabidopsis mutants. The heat map represents hierarchical clustering data obtained from the quantification of sugars by sequential extraction of outer mucilage with 0.05 M hydrochloric acid (30 min at 85°C, gentle shaking) followed by 0.2 M sodium hydroxide (15 min at room temperature, gentle shaking) labeled in black and inner mucilage sugars by RGase digestion (16 h at 40°C, gentle shaking) labeled in red. Mean values from two biological replicates were normalized, and the color of each block in the map reflects the relative amount of each sugar (from −2 in black to the highest values in white). All genotypes are in the Ws accession. WT, Wild type.

In vitro binding assays could not be carried out directly on water-extracted outer mucilage, as Xyl contents were very low. The very high viscosity of these extracts precluded the preparation of sufficiently concentrated solutions for further reliable quantification of Xyl after incubation with cellulose. Intensive hydrolysis of water-extracted mucilage with RGase prior to ethanol precipitation was tested as a possible method to recover Xyl-enriched fractions. In wild-type Col-2 mucilage extracts, approximately 90% of the Rha and GalA were recovered in the ethanol-soluble fraction, together with most of the Ara and Glc and part of the Man and Gal (Supplemental Fig. S1). GlcA was not detected in either the ethanol-soluble fraction or in the ethanol precipitate. Most of the Xyl was recovered in the ethanol precipitate, suggesting that Xyl residues are present in relatively long structures prone to ethanol precipitation. For *mum5-1*, the distribution of sugars between the ethanol-soluble fraction and the ethanol precipitate was similar to that of wild-type Col-2 mucilage, except for Xyl, which was recovered mainly in the ethanol-soluble fraction (Supplemental Fig. S1). The ethanol precipitates were recovered in small amounts and were difficult to resolubilize. To remedy this, water-extracted mucilage was only partially hydrolyzed with RGase (3 h) prior to ethanol precipitation. The ethanol precipitate fraction obtained after 3 h of RGase treatment of the water-extracted mucilage from wild-type Col-2 was easily resolubilized, and when analyzed for sugar contents it contained 32.5 mol % Rha, 46.1 mol % GalA, and was enriched in Xyl (13.3 mol %; Fig. 4A) compared with the initial water-extracted mucilage. Low amounts of Ara (less than 1 mol %), Man (1.8 mol %), Gal (2.9 mol %), and Glc (2.2 mol %) also were detected. In contrast, the *mum5-1* ethanol precipitate had higher proportions of Rha (42.7 mol %) and GalA (52.3 mol %) and was enriched only slightly in Xyl (3.3 mol %) compared with the initial water-extracted mucilage. Low levels (less than 1 mol %) of Ara, Man, Gal, and Glc also were detected.

Linkage analysis was performed on wild-type Col-2 and *mum5-1* ethanol precipitates obtained after treating water-extracted mucilage for 3 h with RGase (Table II). In agreement with the major domain of water-extracted mucilage being unbranched RG-I, the majority of Rha was (1,2)-linked in both *mum5-1* and the wild type, although these were enriched in the mutant, as they were present in a higher proportion. The remaining Rha in wild-type tailored mucilage extracts was either (1,2,4)-linked (8%), indicating a small amount of substituted RG-I, or terminal units (7%). In contrast, only very low amounts of (1,2,4)-linked Rha units were present in *mum5-1* precipitates, in comparison with the wild type, indicating a strong reduction in RG-I branching in *mum5-1*. The RG-I backbone had a similar DP in both mutant and the wild type and was calculated as 26. The presence of branched xylans was indicated in wild-type Col-2 by (1,4)-linked residues, with some (1,2,4)-linked Xyl residues; however, in *mum5-1*, (1,4)-linked Xyl was reduced and represented only 5.4 mol% of total neutral sugars. RG-I branched at low levels, branched xylan chains, and low amounts of other polymers such as galactoglucomannans and xyloglucan also are likely to be present in Arabidopsis mucilage (Voiniciuc et al., 2015c). In agreement, significant amounts of t-Xyl, t-Gal, (1,4,6)-Man, (1,4)-linked Glc, and (1,4,6)-linked

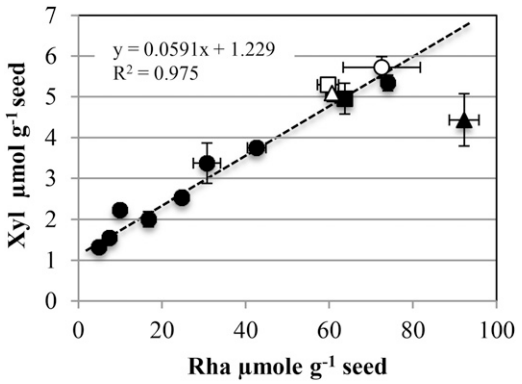

Figure 3. Rha and Xyl contents of the outer HCl-NaOH-extracted mucilage layer are tightly proportional except in *mum5*. White circle, Wild-type Ws; black circles, *gl2*, *mum1*, *mum2*, and *sbt1.7* mutants (Ws accession); white square, wild-type Col-0; black square, *cesa5-2* (Col-0 accession); white triangle, wild-type Col-2; black triangle, *mum5* (Col-2 accession). Values are means of two biological repeats ± SD.

Table I. *Monosaccharide composition of seed mucilage extracted from cesa5 and mum5 compared with the wild type*

Intact seeds were extracted sequentially with 0.05 M HCl and 0.3 M NaOH, RGase, and Maxazyme. Values (mg g^{-1} intact dry seeds ± SD) are shown for two independently extracted samples from two biological repeats. n.d., Not detected.

Monosaccharide	Wild-Type Col-0	*cesa5-2*	Wild-Type Col-2	*mum-5-1*
HCl-NaOH				
Rha	8.72 ± 0.367	9.84 ± 0.350	8.86 ± 0.219	13.47 ± 0.519
Fuc	n.d.	n.d.	n.d.	n.d.
Ara	2.43 ± 0.030	2.08 ± 0.041	2.29 ± 0.146	3.44 ± 0.056
Xyl	0.70 ± 0.005	0.65 ± 0.050	0.67 ± 0.028	0.58 ± 0.085
Man	0.29 ± 0.054	0.20 ± 0.037	0.21 ± 0.005	0.30 ± 0.028
Gal	0.76 ± 0.026	0.72 ± 0.030	0.62 ± 0.029	0.77 ± 0.026
Glc	2.28 ± 0.341	2.03 ± 0.066	1.95 ± 0.067	2.54 ± 0.230
GalA	13.97 ± 0.160	17.95 ± 0.072	10.89 ± 1.153	16.33 ± 0.149
Total	29.15 ± 0.552	33.47 ± 0.333	25.49 ± 1.199	37.44 ± 0.462
RGase				
Rha	3.99 ± 0.170	1.82 ± 0.047	3.82 ± 0.091	1.67 ± 0.251
Fuc	n.d.	n.d.	n.d.	n.d.
Ara	1.55 ± 0.051	1.26 ± 0.017	1.86 ± 0.264	2.21 ± 0.197
Xyl	n.d.	n.d.	n.d.	n.d.
Man	0.26 ± 0.049	0.22 ± 0.027	0.26 ± 0.031	0.31 ± 0.023
Gal	0.38 ± 0.039	0.35 ± 0.014	0.34 ± 0.095	0.33 ± 0.075
Glc	0.43 ± 0.018	0.47 ± 0.014	0.28 ± 0.047	0.17 ± 0.033
GalA	5.11 ± 0.051	2.26 ± 0.032	4.99 ± 0.058	1.92 ± 0.081
Total	11.72 ± 0.377	6.38 ± 0.098	11.56 ± 0.249	6.61 ± 0.595
Maxazyme				
Rha	0.27 ± 0.018	0.19 ± 0.003	0.31 ± 0.021	0.23 ± 0.036
Fuc	0.15 ± 0.017	0.10 ± 0.004	0.18 ± 0.009	0.18 ± 0.014
Ara	0.68 ± 0.021	0.45 ± 0.019	0.74 ± 0.003	0.86 ± 0.056
Xyl	0.89 ± 0.038	0.62 ± 0.002	1.15 ± 0.130	1.27 ± 0.126
Man	0.40 ± 0.028	0.31 ± 0.000	0.45 ± 0.005	0.51 ± 0.056
Gal	1.32 ± 0.002	1.12 ± 0.027	1.38 ± 0.053	1.44 ± 0.093
Glc	4.53 ± 0.017	3.21 ± 0.149	5.22 ± 0.562	5.86 ± 0.789
GalA	0.37 ± 0.009	0.20 ± 0.013	0.48 ± 0.330	0.33 ± 0.043
Total	8.61 ± 0.057	6.21 ± 0.206	9.90 ± 0.816	10.68 ± 1.213

Gal also were detected in wild-type Col-2 ethanol precipitates. Interestingly, these residues also were reduced in *mum5-1* tailored mucilage.

The ethanol-precipitated fractions obtained after 3 h of RGase treatment of outer mucilage extracts were tested for their ability to bind to fibrillated primary cell wall cellulose. For the wild-type Col-2 fraction, 10 to 12 μg of Rha, Xyl, and GalA was able to adsorb onto 1 mg of cellulose, which corresponded to 30%, 82%, and 22% of the Rha, Xyl, and GalA initially present, respectively (Fig. 4B). This indicated not only that xylan chains strongly adsorb onto cellulose but also mediate the adsorption of some RG-I oligomers, in agreement with a covalent linkage between xylan and RG-I chains. In contrast, *mum5-1* ethanol precipitates exhibited very weak adsorption to cellulose, with only approximately 2 μg of Rha, Xyl, and GalA able to adsorb onto 1 mg of cellulose, which corresponded to 4%, 45%, and 4% of the Rha, Xyl, and GalA initially present, respectively. Although the very low amounts of Xyl present in the fraction were able to adsorb onto cellulose to a certain extent, RG-I stretches did not appear to be associated with these. The very low amounts of Xyl present in *mum5* soluble mucilage could reflect the presence of small amounts of independent Xyl-containing polymers such as heteroxylans or xyloglucans.

Enzymatically Tailored Water-Extracted Mucilage from Wild-Type Col-0 Adsorbs to Cellulose in Vitro with High Affinity via Xylan Side Chains

Outer mucilage was extracted from seeds of the reference accession wild-type Col-0, treated for 3 h with RGase, and precipitated with ethanol. A solution of the ethanol-precipitated fraction was prepared at a set volume for three concentrations and then mixed with a set volume of water or cellulose microfibrils in suspension. After incubation, sugar analyses were performed on the supernatants recovered, and the amounts of each major individual sugar (GalA, Rha, and Xyl) were determined. The initial concentration of unbound sugars was determined from the sample with water alone and compared with the concentration of unbound sugars in samples with cellulose. The amount of bound material (total and individual sugars) per mass of

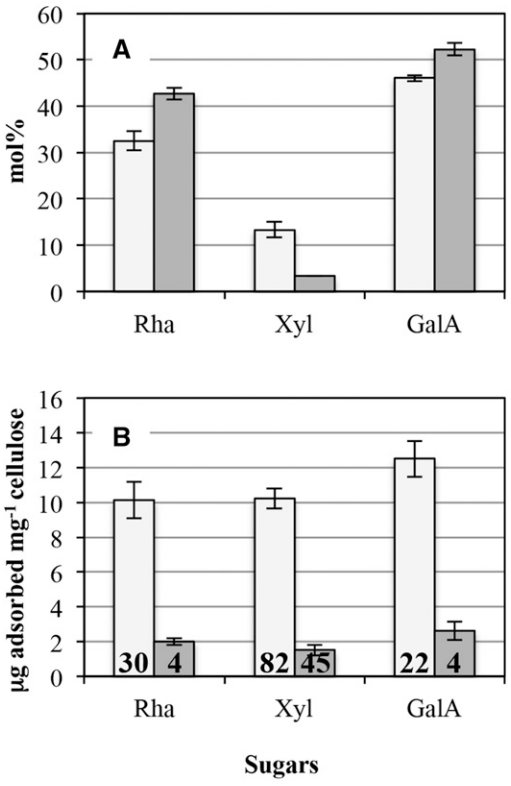

Figure 4. Sugar contents in enzymatically tailored water-extractable mucilage. Water-extracted mucilage was partially degraded with RGase (3 h) and then precipitated with ethanol. The ethanol precipitate was recovered as enzymatically tailored water-extractable mucilage. A, Enzymatically tailored water-extracted mucilage from wild-type Col-2 (light gray bars) was enriched in Xyl compared with *mum5-1* (dark gray bars). Results are given as average mol % ± SD of three technical replicates. B, Enzymatically tailored water-extracted mucilage from wild-type Col-2 (light gray bars) was able to bind to cellulose in vitro, unlike that of *mum5-1* (dark gray bars). Mean values of each sugar bound per mg of cellulose are shown ± SD of two technical replicates. The percentage of each sugar that was bound to cellulose is indicated within the bars.

cellulose was then calculated. Rha, Xyl, and GalA were adsorbed onto cellulose at all three concentrations used (Supplemental Table S3), so the binding assay was repeated over a larger range of concentrations, including concentrations high enough to approach cellulose surface saturation to gain further insight into the binding mechanism. Large amounts of enzymatically tailored water-extracted mucilage (ethanol-precipitated fractions after 3 h of RGase treatment) were prepared from seeds of a biological replicate of wild-type Col-0. The ethanol-soluble fraction, which represented approximately 80% by weight of the initial water-soluble mucilage, contained more than 98 mol% Rha and GalA in a molar ratio close to 1 (Supplemental Fig. S2). The ethanol precipitate was similar to that of wild-type Col-2 (Table II), with 27 mol% Rha, 42 mol% GalA, and 19 mol% Xyl (Supplemental Fig. S2). Minor amounts of Ara, Man, Gal, and Glc also were detected (data not shown).

The ethanol-soluble fraction and the ethanol-precipitated fraction were tested for their ability to bind to fibrillated primary cell wall cellulose. The binding capacity of polymers to cellulose is presented as binding isotherms (Fig. 5), where the mass of bound material (total sugars or individual sugars) per mass of cellulose is plotted versus the concentration of free material remaining in solution at equilibrium concentration. From binding isotherms for total sugars, the ethanol precipitate was clearly observed to adsorb to cellulose in vitro, whereas the ethanol-soluble fraction did not bind to cellulose at all (Fig. 5A). As classically observed for a Langmuir adsorption mechanism, concentration influenced adsorption and a plateau was reached at saturation, which corresponded to the maximum adsorption capacity. Plotting binding isotherms individually for each of the main sugars (Rha, GalA, and Xyl) in the ethanol precipitate confirmed that Xyl strongly adsorbs onto the cellulose surface (Fig. 5B). Indeed, the amount of Xyl remaining in solution after incubation of mucilage ethanol-precipitated fraction solutions with cellulose was very low, even for the highest concentrations of solutions used, so that a plateau was not reached in our experimental conditions. Additionally, part of the Rha and GalA present in the ethanol precipitate also was adsorbed to cellulose (Fig. 5B), while Rha and GalA present in the ethanol-soluble fraction were not (Fig. 5A). This confirmed that the xylan chains mediate the adsorption of RG-I scaffold stretches to which they are attached, since unsubstituted RG-I oligomers were unable to adsorb to

Table II. *Linkage analysis of tailored seed mucilage extracted from mum5-1 compared with the wild type*

Wild-type Col-2 and *mum5-1* water-extracted mucilage was partially degraded with RGase (3 h) and then precipitated with ethanol. Values (average mol % of neutral sugars) are shown two technical repeats, with variance less than 7% for all samples. Values are scaled to direct neutral sugar analysis (Fig. 4A). tr., Trace.

Sugar and Linkage	Wild-Type Col-2	*mum5-1*
Rha		
t-Rha*p*	4.33	6.62
2-Rha*p*	50.99	82.07
2,4-Rha*p*	4.88	0.81
Ara		
t-Ara*f*	0.16	0.10
3-Ara*f*	1.24	0.99
Xyl		
t-Xyl*p*	5.78	0.84
4-Xyl*p*	14.67	5.40
2,4-Xyl*p*	4.25	0.77
Man		
4,6-Man*p*	3.30	tr.
Gal		
t-Gal*p*	3.69	0.66
3-Gal*p*	0.72	tr.
4,6-Gal*p*	0.99	0.66
Glc		
4-Glc*p*	3.10	1.09
4,6-Glc*p*	1.00	tr.

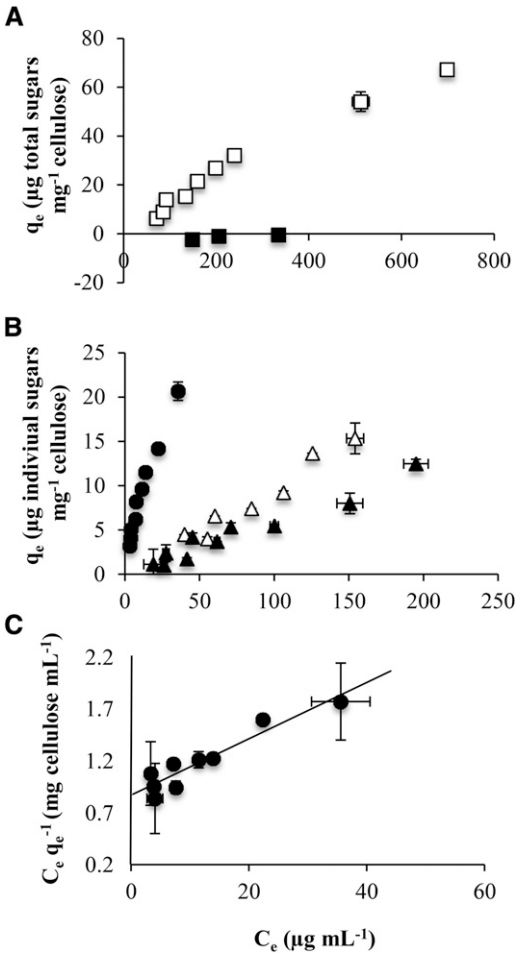

Figure 5. Adsorption isotherms of enzymatically tailored water-extracted mucilage from wild-type Col-0. Water-extracted mucilage was partially degraded with RGase (3 h) and then precipitated with ethanol. The ethanol precipitate was recovered as enzymatically tailored mucilage. The mass of bound material per mass of cellulose (q_e) and the concentration of free material remaining in solution at equilibrium concentration (C_e) were quantified. Values are means ± SD of two technical replicates. A, Binding isotherms show that, in contrast to the ethanol-soluble fraction (black squares), the ethanol precipitate (white squares) is able to bind to cellulose in vitro. B, Binding isotherms for each of the main individual sugars (Rha, GalA, and Xyl) in the ethanol precipitate show that Xyl strongly adsorbs onto the cellulose surface (black circles), with Rha (black triangles) and GalA (white triangles) binding more weakly. C, A linearized form of the Langmuir model was applied to the Xyl-binding isotherm experimental data shown in B. A maximum adsorption capacity of 37 μg Xyl mg^{-1} cellulose and an adsorption constant of 0.0311 mL μg^{-1} Xyl were determined, corresponding to a modest maximum adsorption capacity but a very high affinity of the polymer for cellulose.

cellulose by themselves. To quantify the adsorption mechanism of xylan onto cellulose, a linearized form of the Langmuir model (Langmuir, 1918) was applied to the Xyl-binding isotherm experimental data. As shown in Figure 5C, it was possible to fit a linear model function to data with an r^2 of 0.89. A maximum adsorption capacity of 37 μg Xyl mg^{-1} cellulose and an adsorption constant of 0.0311 mL μg^{-1} Xyl were determined, which confirmed the high affinity of xylan branches for cellulose.

Xylan Epitopes Are Localized in Adherent Mucilage Regions with Diffuse Cellulose

Adherent mucilage has been shown previously to exhibit domains that differ in their structure and constituent polysaccharides (Willats et al., 2001; Blake et al., 2006; Macquet et al., 2007a; Young et al., 2008). Notably, cellulose is observed in wild-type mucilage as intense rays that span from the tops of columella to the edge of adherent mucilage combined with diffuse labeling between rays (Fig. 6, A, C, and D; Macquet et al., 2007a). To determine where xylan was localized in adherent mucilage, the AX1 antibody, which recognizes unsubstituted 1,4-β-D-xylosyl oligosaccharides (Guillon et al., 2004), was used in whole-mount immunolocalization. Wild-type Col-2 mucilage was labeled with AX1 in a region from above the columella to the outer edge and was excluded from regions with cellulose rays (Fig. 6, A, B, and D). Furthermore, immunolabeling of the *pmei6-1* mutant, which is defective for the fragmentation of the outer primary cell wall, confirmed that AX1 was labeling xylan in mucilage and not cell wall fragments (Supplemental Fig. S3). AX1 labeling of *mum5-1* mucilage was greatly reduced, although some was still visible colocalized with the cellulose rays (Fig. 6, E–H), suggesting that the *mum5-1* mutant is leaky or that the *MUM5* function is redundant with that of another gene.

MUM5 Encodes a Putative Xylosyl Transferase

The gene affected in *mum5-1* remained to be identified, although it had been indicated previously to be a pectin methylesterase (M. Facette and C. Somerville, personal communication [cited in Western, 2006]). We mapped the *mum5-1* mutation to a region of 6.68 Mb on the upper arm of chromosome 3 using linkage analysis to molecular markers. Analysis of data obtained by whole-genome resequencing of wild-type Col-2 and *mum5* genomic DNA identified 137 polymorphisms unique to the mutant in the interval. Of these, only 34 were predicted to generate stop or nonsynonymous codons or frameshift mutations. The gene At3G10320 was highlighted as a likely candidate for the *MUM5* gene, as it was annotated as a glycosyl transferase family 61 protein, which are classed by the Carbohydrate-Active Enzymes database (http://www.cazy.org/) as β-1,2 xylosyl transferases. This gene contained a C-to-T point mutation in the open reading frame that changed Ala-387 to Thr (Fig. 7A), and although considered a conservative mutation, it has been documented previously to cause defective protein function, probably due to physical differences (Yanagisawa et al., 2001; Podoly et al., 2010). The At3G10320 gene was annotated recently as *MUCILAGE-RELATED21* and shown to be required for the synthesis of branched xylan in seed coat

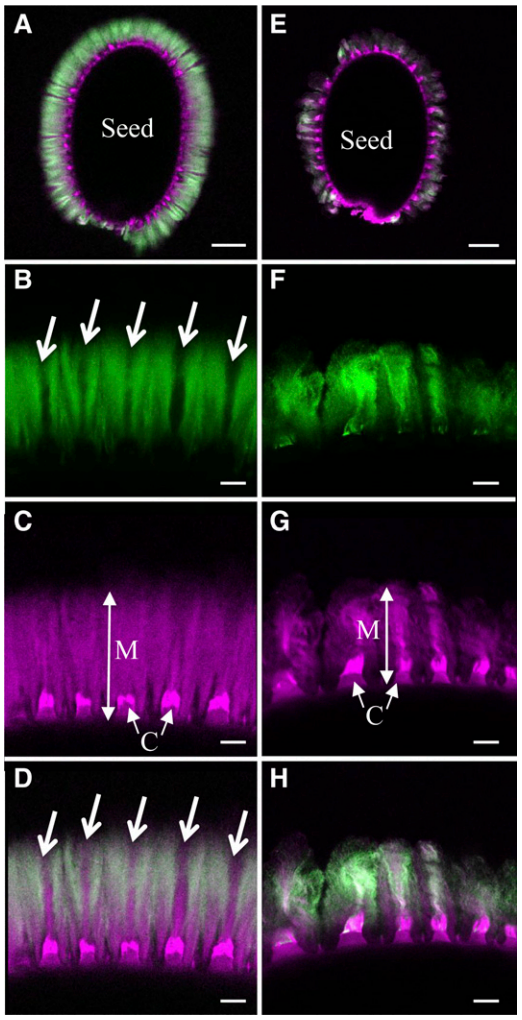

Figure 6. Labeling of xylan in adherent mucilage released from wild-type and *mum5-1* seeds. Confocal microscopy optical sections show adherent mucilage released from mature imbibed seeds after labeling of xylan epitopes with AX1 antibody (green) or staining of cellulose with Pontamine Fast Scarlet 4B (magenta). A to D, Wild-type Col-2 seeds. E-H, *mum5-1* seeds. A and E show whole seeds, and B, C, and D or F, G, and H show higher magnifications of mucilage from the same seeds, respectively. A, D, E, and H show composite images of double labeling with Pontamine and AX1 antibody. Arrows indicate zones in adherent mucilage that are not labeled with AX1. C, Columella; M, adherent mucilage. Bars = 100 μm (A and E) and 20 μm (B–D and F–H).

epidermal cells (Voiniciuc et al., 2015a). Furthermore, available in silico data and quantitative reverse transcription-PCR analysis indicated that *MUM5/MUCI21* was expressed specifically in the seed coat when the embryo was at the linear cotyledon and mature green stages (Supplemental Fig. S4; Le et al., 2010; Voiniciuc et al., 2015a). This expression pattern is similar to those of other genes, such as *CESA3*, *CESA5*, and *MUM4/RHM2*, which encode enzymes involved in the production of mucilage. Two independent mutants with insertions in At3G10320 were obtained (Fig. 7A), and mucilage released from their

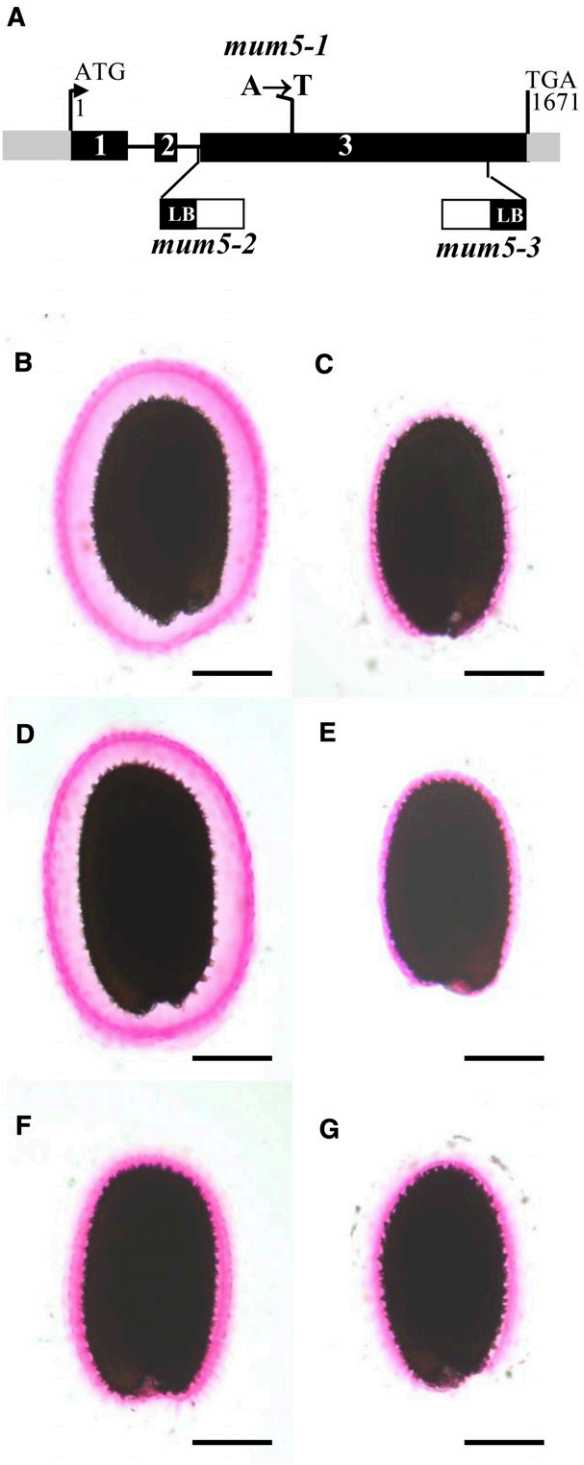

Figure 7. Mutants in the MUM5 putative xylosyl transferase have a reduced adherent mucilage layer. A, Schematic representation of the structure of *MUM5* as annotated by The Arabidopsis Information Resource (http://www.arabidopsis.org/). The positions and nature of *mum5-1* mutations and the sites and orientation of *mum5-2* and *mum5-3* insertions are indicated. LB, Left border. B to G, Visualization of the adherent mucilage layer by ruthenium red staining of seeds from wild-type Col-2 (B), *mum5-1* (C), wild-type Col-0 (D), *mum5-2* (E), *mum5-3* (F), and F1 seed coat/F2 seed from a cross between *mum5-1* and *mum5-2* (G). Bars = 200 μm.

seeds was examined by ruthenium red staining (Fig. 7, E and F). Seeds from both mutants had reduced adherent mucilage layers compared with wild-type seeds (Fig. 7, A and D), similar to *mum5-1* seeds. To confirm that they were mutant alleles of *mum5-1*, crosses were performed between the different mutants, and mucilage released from F1 seed coats of F2 seeds was examined by ruthenium red staining. A reduced adherent mucilage layer was observed in all cases (Fig. 7G; data not shown). This genetic noncomplementation confirmed that At3G10320 was *MUM5* and that the insertion mutants were indeed mutant alleles, so they were named *mum5-2* and *mum5-3* accordingly.

A gentle water extraction of mucilage was carried out on seeds from *mum5-1*, *mum5-2*, and *mum5-3* and their corresponding wild type. This gentle water extraction was followed by RGase digestion of the inner mucilage layer. A clear and similar redistribution of the inner to the outer layer was observed for the three alleles (Table III). In both wild-type accessions, the proportion of outer mucilage (calculated on a GalA basis) was calculated to be 69%, whereas in *mum5-1*, *mum5-2*, and *mum5-3*, this represented 85% ± 1%. Interestingly, the Rha-Xyl ratio was more drastically increased in *mum5-2* and *mum5-3* water-extractable mucilage compared with wild-type Col-0 (+236% and +275%, respectively) than in *mum5-1* water-extractable mucilage compared with wild-type Col-2 (+189%).

DISCUSSION

Interactions between cellulose, hemicelluloses, and pectin are key determinants of plant cell wall properties and function. Much remains to be understood concerning these interactions, and studies are often hampered by the difficulty of isolating individual components for physicochemical studies. Seed mucilage is a relatively simple and easily accessible mixture of polysaccharides that is becoming an important model for studying these polymers. Two layers of mucilage are released from Arabidopsis seeds, an outer diffuse layer that can be easily removed by agitation and an inner layer that remains attached to the seed coat. Cellulose has been clearly demonstrated to mediate the adherence of inner mucilage RG-I to the seed surface (Harpaz-Saad et al., 2011; Mendu et al., 2011; Sullivan et al., 2011; Ben-Tov et al., 2015; Griffiths et al., 2015), but the exact mechanism remained to be defined. Determining the relationship between the outer and the inner layers should contribute to our understanding of the interactions involved, and it can be hypothesized that two key points are necessary for the partitioning of polysaccharides into two layers: (1) a correctly constructed cellulose scaffold; and (2) mucilage pectin with an appropriate structure and properties for both interaction with cellulose and hydration.

Disruption of the formation of the cellulosic rays in mucilage has systematically been associated with a redistribution of RG-I from the inner to the outer layer, in agreement with cellulose-pectin interactions (Harpaz-Saad et al., 2011; Mendu et al., 2011; Sullivan et al., 2011; Ben-Tov et al., 2015; Griffiths et al., 2015). Mechanisms through which such interactions could occur have been suggested to consist of noncovalent bonding between cellulose and RG-I side chains (Haughn and Western, 2012). This is based on the fact that, while most of the RG-I backbone is unbranched in the outer mucilage layer, more complex branched pectin molecules together with some hemicelluloses are found in the inner layer, and these may adhere to the cellulose framework. This is, however, hard to prove, since the inner adherent layer is difficult to extract for study as an independent entity. Strong chemicals or procedures involving vigorous shaking have been used for this purpose, and it has been shown that, although mucilage consists primarily of RG-I, it also contains other polymers such as HG, xylans, heteromannans, xyloglucan, and arabinogalactan proteins (Walker et al., 2011; Voiniciuc et al., 2015c). Despite their low abundance, these components could play essential roles in controlling mucilage properties (Voiniciuc et al., 2015c). For example, glucomannans and galactoglucomannans synthesized by CSLA2 and MUCI10 seem to be involved in structuring the adherent layer of mucilage (Yu et al., 2014; Voiniciuc et al., 2015b). Determining how these different polymers are involved in RG-I attachment to cellulose is challenging, and it is unclear which are part of the mucilage itself or originate from fragments of primary cell wall released when the epidermal cells rupture on imbibition. Treatment of intact seeds with RG-I-hydrolyzing enzymes after removal of the outer mucilage layer enables the solubilization of the

Table III. *GalA content and Rha-Xyl molar ratio of seed mucilage extracted from mum5-1, mum5-2, and mum5-3 compared with the wild type*

Intact seeds were extracted sequentially with water and RGase. Values (mg g^{-1} intact dry seeds for GalA and molar ratio for Rha/Xyl ± SD) are shown for three biological repeats.

Plant	GalA Outer Layer	GalA Inner Layer	Rha/Xyl Outer Layer
Wild-type Col-2	12.76 ± 0.489	5.87 ± 0.093	16.4 ± 0.50
mum5-1	15.48 ± 0.575	2.66 ± 0.003	31.2 ± 0.27
Wild-type Col-0	13.91 ± 0.441	6.24 ± 0.031	16.1 ± 0.30
mum5-2	16.24 ± 0.332	2.55 ± 0.008	38.1 ± 1.35
mum5-3	14.31 ± 0.769	2.66 ± 0.005	44.3 ± 1.73

depolymerized inner layer of RG-I, but not polymers that interact strongly with cellulose. An alternative for gaining insight into the polymers present in the adherent layer, as shown here, is a detailed characterization of outer layer polysaccharides, as a minor component of outer mucilage has been hypothesized to originate from the adherent mucilage layer (Macquet et al., 2007a). This component was precipitated with ethanol and contained around 10% of the outer mucilage RG-I and the majority of the Xyl residues (Supplemental Fig. S1, A and B).

Analysis of the composition of the outer layer of mucilage in a series of mutant alleles demonstrated a tight proportionality of Xyl-GalA-Rha (Fig. 2), in accord with increasing evidence for a connection between pectin and xylan synthesis (Atmodjo et al., 2013). Linkage analysis of the ethanol precipitate from outer mucilage identified xylan linkages, in agreement with xylan side chains covalently linked to the RG-I backbone (Table II), similar to those observed in polysaccharides isolated from leaves of *D. kaki* and from Arabidopsis suspension culture medium (Duan et al., 2004; Tan et al., 2013). In vitro binding assays showed that, while unbranched RG-I oligomers did not bind to cellulose, a Xyl-enriched mucilage fraction did (Fig. 5A). Moreover, in the latter fraction, a proportion of the Rha and GalA residues, in addition to most of the Xyl, were bound to cellulose. If Xyl-containing polymers and RG-I were independent one from another, Rha and GalA residues would not bind to cellulose. This demonstrates that mucilage RG-I has xylan branches, which can mediate the adsorption of mucilage onto cellulose in vitro through noncovalent linkages and, thus, could fix mucilage RG-I to cellulose in adherent mucilage.

The adsorption constant value observed for these RG-I-attached xylan chains is very close to that determined experimentally for xyloglucan adsorption onto bacterial microcrystalline cellulose (Lopez et al., 2010), highlighting that both polymers show a similar very high affinity for cellulose. Xylan affinity for cellulose has been observed previously in quince (Cydonia oblonga) seed mucilage, which is constituted of highly branched, partially acetylated 4-*O*-methyl-glucuronoxylans coating individual cellulose microfibrils (Lindberg et al., 1990). Acidic glucuronoxylans act as biological surfactants, giving each cellulose microfibril a net negative repulsive surface charge, which prevents them from flocculating. Microfibrils can be organized into remarkable helical arrays that are very similar to those of cholesteric liquid crystals (Abeysekera and Willison, 1988, 1990; Reis et al., 1991). The occurrence of mucilage cellulose being solubilized through interactions with negatively charged polysaccharides was suggested in the pioneering work of Mühlethaler (1950). In flaxseed (*Linum usitatissimum*) mucilage, when the so-called polyuronide was hydrolyzed by sulfuric acid, cellulose microfibrils were shown to associate and precipitate as a fibrous insoluble residue (Mühlethaler, 1950). More recently, it was proposed that fractions of the arabinoxylan and RG-I in flaxseed mucilage are associated through covalent interactions, which enhances their viscosity (Naran et al., 2008). The solubilization of cellulose in Arabidopsis mucilage through interactions with xylan branches on RG-I is corroborated by the localization of xylan epitopes within seed mucilage. These were excluded from regions where cellulose was observed as rays (Fig. 6, A, B, and D), the rays being microfibrils of birefringent crystalline cellulose (Sullivan et al., 2011). In contrast, they were abundant in the regions occupied by diffuse nonrefractive cellulose (Fig. 6D). The exact chemical structure of the xylan moieties attached to RG-I cannot be deduced from the linkage analysis. The total ratio of residues singly branched at O-2 to unbranched residues in the xylan backbone was relatively low (0.29:1; Table II), and, since GlcA and t-Ara were rare if not absent, it is unlikely that there is glucuronoarabinoxylan or arabinoxylan. A portion of the more abundant t-Gal and t-Xyl residues, therefore, is likely to constitute side group residues of the xylan backbone, as suggested previously for flax (Naran et al., 2008).

In *mum5* mutants, RG-I is redistributed to the outer mucilage layer (Table III; Macquet et al., 2007a), despite cellulose still being present in the adherent layer (Table I; Fig. 6, G and H). This suggested that mucilage adhesion is affected in the mutant due to differences in the branching or cross-linking of other mucilage polysaccharides (Western et al., 2001; Macquet et al., 2007a). In contrast to other mucilage mutants, the ratio of Rha to Xyl in the outer mucilage of *mum5* mutants was much higher (Table III; Fig. 3), indicating a defect in the addition of Xyl branches to RG-I. This was confirmed by the significant reduction in (1,2,4-)-linked Rha and (1,4)-linked Xyl in enzymatically tailored mucilage extracts from *mum5-1* compared with the wild type (Table II). Xylan epitopes within adherent mucilage also were reduced in the mutant (Fig. 6F). Furthermore, enzymatically tailored mucilage extracts from *mum5-1* had dramatically reduced binding to cellulose in vitro compared with the wild type. Taken together, the mutant phenotypes confirm that the affinity of Xyl branches for cellulose is responsible for the adhesion of mucilage RG-I. It was proposed previously that the high-M_w macromolecular population of polymers in outer mucilage separated by HP-SEC was part of the adherent layer (Macquet et al., 2007a). This population was absent from *mum5-1* extracts (Sullivan et al., 2011), which have less Xyl in their ethanol-precipitated fraction of outer mucilage (Supplemental Fig. S1), and thus confirms that these polymers are representative of those in the adherent layer. This provides important information about how mucilage layers are formed: during seed development, both unbranched and Xyl-branched RG-I populations are secreted into the apoplast; however, part of the Xyl-branched RG-I is released into the outer layer on imbibition, probably because it does not come into contact with cellulose microfibrils.

The causal mutation in *mum5-1* was identified in a gene annotated as a xylosyl transferase (Fig. 7A). These enzymes synthesize polysaccharides by the transfer of

Xyl residues from a nucleotide sugar to an oligosaccharide or polysaccharide acceptor (Mohnen, 2008). The predicted activity of MUM5 is thus in agreement with the reduced levels of Xyl branches on RG-I in mutant mucilage. In a recent study, this gene was implicated in the addition of xylan branches to mucilage polysaccharides and termed *MUCI21* (Voiniciuc et al., 2015a). Furthermore, in silico expression data and analyses of transcript abundance indicate strong expression in the seed coat, similar to other enzymes involved in the synthesis of mucilage polysaccharides (Supplemental Fig. S4; Voiniciuc et al., 2015a). Glycosyl transferases involved in pectin synthesis are type II membrane proteins localized in the Golgi membrane with their catalytic site facing the lumen. In accordance, the hydropathy profile of MUM5 indicates a potential transmembrane domain in the N-terminal region of the protein, and Voiniciuc et al. (2015a) localized MUM5/MUCI21-sYFP to the Golgi. Xylan epitopes were still observed in the mucilage of *mum5-1*, indicating that this mutant could be leaky or functionally redundant with another xylosyl transferase. Comparison of the sugar composition of mucilage extracts from two other *mum5* alleles resulting from T-DNA insertions in the gene indicated that the increase in the ratio of Rha to Xyl was greater in the insertion mutants, in accord with *mum5-1* being a weaker mutant allele with a causal mutation producing a conserved amino acid change (Fig. 7A). The glycosyl transferase IRX14 also has been implicated in the production of xylan, and *irx14* mutants have almost no adherent mucilage (Voiniciuc et al., 2015a). It was proposed that IRX14 synthesizes a linear xylan backbone to which xylan branches are added by MUM5/MUCI21, with the branches required for pectin attachment to the seed surface and the xylan backbone maintaining cellulose distribution. Based on the results presented here that implicate MUM5/MUCI21 in the addition of Xyl branches to RG-I, an alternative is that IRX14 participates in the extension of xylan from the Xyl branches on RG-I.

The binding affinity of Xyl ramifications on RG-I to a cellulose scaffold is not the only factor involved in the formation of the adherent mucilage layer. The SOS5 fasciclin-like arabinogalactan protein also has been implicated in pectin adhesion through a mechanism independent of cellulose (Griffiths et al., 2014). In effect, *sos5* mutants have modified partitioning of mucilage polysaccharides, similar to *cesa5* and *mum5*, with a more severe loss of adherence in *cesa5 sos5* mutants. SOS5 is thought to influence pectin-mediated adherence, as it alters the pectin defects of *fly1* and *mum2* mutants (Griffiths et al., 2014). Therefore, in addition to Xyl branching of RG-I, other pectin modifications also would appear to influence adherence, and these remain to be characterized. Glucomannans and galactoglucomannans can interact with cellulose and appear to participate in the organization and crystallization of mucilage cellulose (Yu et al., 2014; Voiniciuc et al., 2015b). *csla2* and *muci10* mutants affected in glucomannan and galactoglucomannan synthesis have more densely packed adherent layer polymers, with a small repartitioning of RG-I to the outer mucilage layer. Voiniciuc et al. (2015b) proposed that galactoglucomannan serves as a scaffold around the cellulosic rays that control mucilage density. This would involve interactions between galactoglucomannan and cellulose and, probably, other mucilage polymers. Cellulose observed on direct staining of *irx14* mucilage was lost when seeds were shaken, which was not the case in *mum5/muci21* (Voiniciuc et al., 2015a), which suggests that IRX14 synthesizes xylan in polymers other than RG-I branches, which also could interact with cellulose. The loss of cellulose staining coupled with the severity of the *irx14* pectin redistribution to outer mucilage could be due to impaired anchoring of cellulose to the seed surface in the absence of xylan synthesized by IRX14. Finally, calcium cross-links between HG also would appear to influence adherent mucilage density, as imbibition of wild-type mucilage in EDTA increases the size of this layer (Rautengarten et al., 2008; Arsovski et al., 2009; Saez-Aguayo et al., 2013). The identification here of a novel link between RG-I and cellulose through Xyl branches opens up new perspectives for our understanding of how cell wall polymers interact and form cell wall architecture.

MATERIALS AND METHODS

Plant Material

Arabidopsis (*Arabidopsis thaliana*) plants were grown in either a growth chamber (photoperiod of 16 h of light at 21°C and 8 h of dark at 18°C, 65% relative humidity, and 170 μmol m^{-2} s^{-1}) or a glasshouse (18°C–28°C) with a minimum photoperiod of 13 h ensured when required by supplementary lighting. Plants were grown in compost (Tref Substrates) and watered with Plan-Prod nutritive solution (Fertil; http://www.plantprodsolutions.com/). Seeds for biochemical analyses were produced from plants of each genotype grown and harvested together, but biological repeats were not cultivated in parallel.

Mutants affected in mucilage release were isolated from the Institut National de la Recherche Agronomique Versailles collection of T-DNA mutants in the Wassilewskija-4 (Ws-4) accession (Bechtold and Pelletier, 1993). Pools of T3 or T4 lines were sown on 0.5% (w/v) agarose plates and examined after 16 h for the presence of a refractive halo of mucilage around the seed. Seedlings from seeds that did not release mucilage were transplanted to soil for seed production. The resulting plants were noted for the presence or absence of trichomes on leaves and stems. The nonrelease phenotype was verified on the seed lots produced, and their seed color was examined. Four mutants derived from independent pools had normal seed color but had glabrous leaves and stems, so they were crossed to *gl2-6* (SM_3.16350). F1 plants and seed coats showed noncomplementation of the glabrous and mucilage-nonrelease phenotypes, respectively, confirming them to be *gl2* mutant alleles. They were thus named *gl2-7* to *gl2-10*. Three mutants with a *mum2* chemotype had a decreased ratio of soluble to adherent mucilage and increased Gal contents. Two mutants showed noncomplementation of the mucilage-release phenotype in F1 seed coats when crossed with *mum1-1*, and these mutant alleles were renamed *luh-7* and *luh-8*. The third mutant showed noncomplementation of mucilage release in F1 seed coats when crossed with *mum2-11* and was renamed *mum2-15*. Sequencing identified the causal mutation as a 64-bp deletion at the end of the 15th exon, 5,092 bp into the open reading frame, which removes 14 amino acids from the BGAL6 protein. The remaining mutant released mucilage when imbibed in water overnight. When crossed with the *sbt1.7-1* mutant, the mucilage-nonrelease phenotype of this mutant was not complemented in F1 seed coats, showing it to be a new mutant allele that was named *sbt1.7-3*. Sequencing identified the causal mutation to be a 30-bp deletion, 1,762 bp into the open reading frame, which eliminates 10 amino acids from the SBT1.7 protein. *gl2-9*,

gl2-10, *mum2-14*, and *sbt1.7-3* were backcrossed once, and *luh-7* was backcrossed twice, to wild-type Ws-4 prior to biochemical analyses.

Two lines in the Col-0 accession with T-DNA insertions in At3G10320 were identified in the SIGnAL database (Alonso et al., 2003; http://signal.salk.edu); WiscDSLox line 503F10 corresponds to *mum5-2* and SALK _041744 corresponds to *mum5-3*. Seeds from these lines were obtained from the Nottingham Arabidopsis Stock Centre (http://arabidopsis.info). Homozygous lines were obtained using the primers indicated in Supplemental Table S4.

Mucilage Extraction and Tailoring

Outer soluble mucilage was usually extracted from 200 mg of intact seeds with 0.05 M HCl (5 mL) for 30 min at 85°C. After centrifugation (8,000*g* for 5 min), supernatants were carefully removed, and 5 mL of 0.3 M NaOH was added to the seeds. Suspensions were incubated at room temperature with intermittent gentle head-over-tail mixing for 10 min prior to centrifugation (8,000*g* for 5 min). Supernatants were carefully removed, and seeds were rinsed three times with 5 mL of water, acidified to pH 4.5 with 0.05 M HCl, and then rinsed with 5 mL of 50 mM sodium acetate buffer, pH 4.5 (three changes). The extraction supernatants (HCl and NaOH) and first three rinses were combined, filtered through a disposable glass microfiber filter (13 mm diameter, 2.7 μm pore size; Whatman), and retained for analysis after extensive dialysis. RGase (Swiss Prot Q00018; Novozymes) was added to washed seeds (0.8 nkat), and inner adherent mucilage extracts were recovered as described previously (Sullivan et al., 2011). For one series of experiments, wild-type Col-0, *cesa5*, wild-type Col-2, and *mum5-1* seeds were rinsed an additional three times with 5 mL of 50 mM sodium acetate buffer, pH 4.5. Maxazyme (DSM) was added to washed seeds (0.9 nkat), and the reaction was incubated at 40°C for 16 h. After centrifugation (8,000*g* for 5 min), supernatants were removed for analysis. For some experiments, outer soluble mucilage was extracted from 200 mg of intact wild-type Col-0, *mum5-1*, wild-type Col-2, *mum5-2*, and *mum5-3* seeds with water and inner mucilage was extracted with RGase as described previously (Sullivan et al., 2011).

Large-scale extractions were carried using 1 g of seeds and 20 mL of distilled water (wild-type Col-0 culture 1, wild-type Col-2, and *mum5-1*) or 2 g of seeds and 20 mL of distilled water (wild-type Col-0 culture 2) for 3 h at room temperature with gentle head-over-tail mixing. The extracted mucilage was recovered after centrifugation as described above. The three washes were pooled with the extract and filtered on a G2 sintered glass. Aliquots were retained for sugar analysis before freeze drying. Large-scale extractions were performed in triplicate for wild-type Col-0 culture 1, wild-type Col-2, and *mum5-1* and eight times for wild-type Col-0 culture 2.

Freeze-dried water-soluble mucilage aliquots from large-scale extractions were further subjected to digestion with RGase (0.1 nkat g^{-1} freeze-dried mucilage) for 3 h at 40°C or for 16 h at 40°C. Enzyme hydrolysates were precipitated by adding an equal volume of ethanol and incubating overnight at 4°C. The resulting pellets and supernatants were recovered as described previously (Saez-Aguayo et al., 2013).

Glycosyl Residue Composition and Linkage Analysis

Uronic acid (as GalA) was determined by an automated *m*-hydroxybiphenyl method (Thibault, 1979). The difference in response to GlcA and GalA in the presence and absence of sodium tetraborate (Filisetti-Cozzi and Carpita, 1991) was used to quantify them individually in selected fractions. Individual neutral sugars were analyzed as their alditol acetate derivatives (Blakeney et al., 1983) by gas-liquid chromatography after hydrolysis with 2 M trifluoroacetic acid at 121°C for 2.5 h.

Linkage analyses were performed according to Anumula and Taylor (1992) with some modifications. Samples were solubilized in water (1 mg mL^{-1}) and converted into their H^+ form by percolating the solutions through a 1-mL Sigma Dowex 50WX4 resin. Samples were freeze dried and further dried in a vacuum oven at 40°C for 2 h before being dissolved in 0.2 mL of dimethyl sulfoxide. Mixtures were left for 30 min at room temperature with occasional vortexing before adding 0.2 mL of NaOH-dimethyl sulfoxide solution. Methylation was performed with 0.1 mL of methyl iodide for 10 min. The mixture was sonicated and vortexed several times. Two milliliters of water was added, and methylated products were extracted with 2 mL of chloroform. The organic phase was washed three times with 2 mL of water and dried (45°C). Methylated carbohydrates were hydrolyzed with 2 M trifluoroacetic acid and converted to their alditol acetates. The partially methylated alditol acetates were analyzed by gas chromatography-mass spectrometry.

Binding Assays

Solutions of enzymatically tailored water-soluble mucilage (ethanol precipitate of RGase digest for 3 h at 40°C) were prepared at 3 mg mL^{-1} (wild-type Col-0 culture 2) or 1 mg mL^{-1} (wild-type Col-0 culture 1, wild-type Col-2, and *mum5-1*), centrifuged (9,000*g* for 20 min), and filtered through a disposable glass microfiber filter (13 mm diameter, 2.7 μm pore size; Whatman). Wild-type Col-0 culture 1 solution was further diluted to give concentrations of approximately 200, 300, and 500 μg mL^{-1}. Wild-type Col-0 culture 2 solutions were further diluted to give a range of concentration from approximately 300 μg mL^{-1} to approximately 3 mg mL^{-1}. Freeze-dried primary cell wall fibrillated cellulose (Zykwinska et al., 2005) was suspended in distilled water (10 mg mL^{-1}) by Ultra-Turrax treatment (three times 30 s). A total of 925 μL of mucilage solution was added to 500 μg of cellulose suspension and 75 μL of 400 mM sodium acetate buffer, pH 5.8. Controls and blanks were performed by replacing cellulose suspension and mucilage solution, respectively, with identical amounts of distilled water. Samples, including controls and blanks, were incubated 6 h at 40°C with continuous head-over-tail mixing, centrifuged for 20 min at 9,000*g*, and supernatants were carefully removed for direct GalA analysis and individual neutral sugar analysis after trifluoroacetic acid hydrolysis. The amount of adsorbed matter was calculated from the difference in sugar content measured for controls and corresponding cellulose-mucilage blends, taking into account the amount of sugars released by cellulose blanks (average of four measurements). Controls and assays were performed in duplicate.

Langmuir Fit

The adsorption mechanism was quantified using a Langmuir model (Langmuir, 1918), which can be expressed as follows:

$$q_e = \frac{q_m b C_e}{1 + b C_e}$$

where q_e is the mass (μg) of absorbed polymer per mg of cellulose, q_m is the maximum adsorption capacity (μg polymer mg^{-1} cellulose), b is the adsorption constant (mL μg^{-1} polymer), and C_e is the concentration of free polymer remaining in solution at equilibrium (μg mL^{-1}).

The experimental binding isotherm data were further plotted by the linearized form of the Langmuir model with the following equation:

$$\frac{C_e}{q_e} = \frac{1}{b} q_m + \frac{C_e}{q_m}$$

The maximum adsorption capacity was calculated from the slope of line a_1 by $q_m = 1/a_1$ and the adsorption constant from the intercept of line a_2 by $b = 1/(a_2 q_m)$.

Cytochemical Staining and Immunolabeling of Seed Mucilage

Seeds were imbibed in water for 3 h and then rinsed twice prior to staining. The released adherent mucilage was stained with Ruthenium Red or Pontamine Fast Scarlet 4B as described previously (Macquet et al., 2007a; Anderson et al., 2010). The xylan-binding monoclonal antibody AX1 diluted 1:10 was used for immunolabeling (Guillon et al., 2004) with a rat anti-mouse IgG secondary antibody conjugated to Alexa Fluor 488 (Invitrogen). Stained or immunolabeled seeds were observed with a light microscope for ruthenium red (Axioplan 2; Zeiss) or a Leica TCS-SP5-AOBS confocal microscope using a 514- or 488-nm argon laser line to excite Pontamine or Alex Fluor, respectively, and detection of fluorescence emission between 570 and 650 nm or 500 and 550 nm. For comparison of signal intensity within a given experiment, laser gain values were fixed.

Genetic Analyses and DNA Sequencing

The *MUM5* gene was localized to an interval between 851 and 7,538 kb on the upper arm of chromosome 3 using a mapping population of 92 F2 individuals derived from a cross between wild-type Ws-4 and *mum5-1*. DNA was extracted as described by Doyle and Doyle (1990) from flower buds of F2 plants for 11 progeny showing a reduced halo of adherent mucilage on Ruthenium Red staining of F2 seed coats. Genotyping of the individuals was carried out

using the extracted DNA and simple sequence length polymorphism markers and an approximate map position established based on recombination percentages. In parallel, whole-genome resequencing was carried out on wild-type Col-2 and *mum5-1* genomic DNA extracted from leaves by Genome Enterprise (http://www.norwichresearchpark.com/parkdirectory/genomeenterpriselimited.aspx) using an Illumina HiSeq 2000 sequencer. DNA polymorphisms in the mapping interval in the *mum5-1* sequence were identified compared with available wild-type Col-0 sequence (The Arabidopsis Information Resource version 10) and filtered to remove polymorphisms common to wild-type Col-2 using the mutDetect pipeline and fileMatch script developed by the Institut Jean-Pierre Bourgin bioinformatics team (F. Granier, D. Charif and J. Tran, unpublished data).

Statistical Analyses

Data were analyzed in R, a language and environment for statistical computing (R Core Team; http://www.R-project.org/), and combined into a data frame using the dplyr and tidyr packages (http://CRAN.R-project.org/web/packages/dplyr/ and http://CRAN.R-project.org/web/packages/tidyr/). Data were scaled prior to hierarchical ascendant clustering with hclust using either Euclidean distances for genotype clustering or the 1 − Spearman correlation distance for sugar clustering; in both cases, the ward clustering method, ward.D, was employed. Finally, clustered data were plotted as a heat map using the ggdendro and ggplot2 R packages (http://CRAN.R-project.org/web/packages/ggdendro/ and http://CRAN.R-project.org/web/packages/ggplot2/).

Sequence data from this article can be found in The Arabidopsis Information Resource (http://www.arabidopsis.org) database with the locus identifier At3G10320 (*MUM5*).

Supplemental Data

The following supplemental materials are available.

Supplemental Figure S1. Sugar distribution between the ethanol-soluble fraction and ethanol precipitate from wild-type and *mum5-1* water-extracted mucilage after a complete digestion with rhamnogalacturonan hydrolase.

Supplemental Figure S2. Sugar distribution between the ethanol-soluble fraction and ethanol precipitate from wild-type water-extracted mucilage after a short digestion with rhamnogalacturonan hydrolase.

Supplemental Figure S3. AX1 labelling of xylan epitopes is limited to mucilage and is not observed in the primary cell wall.

Supplemental Figure S4. *MUM5* is preferentially expressed in the seed coat during seed development.

Supplemental Table S1. Total sugar amounts in seed mucilage sequentially extracted from *sbt1.7-3*, *gl2-6*, *gl2-7*, *gl2-8*, *gl2-9*, *luh-7*, *luh-8*, and *mum2-15* compared to wild type.

Supplemental Table S2. Monosaccharide composition of water-extracted mucilage.

Supplemental Table S3. Adsorption assays for three concentrations of enzymatically-tailored water-extracted mucilage from wild-type Col-0.

Supplemental Table S4. Sequences of primers used for identification of homozygous mutants.

Received February 11, 2016; accepted March 13, 2016; published March 15, 2016.

LITERATURE CITED

Abeysekera RM, Willison JHM (1988) Development of helicoidal texture in the prerelease mucilage of quince (*Cydonia oblonga*) seed epidermis. Can J Bot **66:** 460–467

Abeysekera RM, Willison JHM (1990) Architecture of the fluid cellulosic arrays in the epidermis of the quince seed. Biol Cell **68:** 251–257

Alonso JM, Stepanova AN, Leisse TJ, Kim CJ, Chen H, Shinn P, Stevenson DK, Zimmerman J, Barajas P, Cheuk R, et al (2003) Genome-wide insertional mutagenesis of *Arabidopsis thaliana*. Science **301:** 653–657

Anderson CT, Carroll A, Akhmetova L, Somerville C (2010) Real-time imaging of cellulose reorientation during cell wall expansion in Arabidopsis roots. Plant Physiol **152:** 787–796

Anumula KR, Taylor PB (1992) A comprehensive procedure for preparation of partially methylated alditol acetates from glycoprotein carbohydrates. Anal Biochem **203:** 101–108

Arsovski AA, Popma TM, Haughn GW, Carpita NC, McCann MC, Western TL (2009) *AtBXL1* encodes a bifunctional β-D-xylosidase/α-L-arabinofuranosidase required for pectic arabinan modification in Arabidopsis mucilage secretory cells. Plant Physiol **150:** 1219–1234

Atmodjo MA, Hao Z, Mohnen D (2013) Evolving views of pectin biosynthesis. Annu Rev Plant Biol **64:** 747–779

Bechtold N, Pelletier G (1993) *In planta Agrobacterium*-mediated transformation of adult *Arabidopsis thaliana* plants by vacuum infiltration. C R Acad Sci II **316:** 1194–1199

Beeckman T, De Rycke R, Viane R, Inzé D (2000) Histological study of seed coat development in *Arabidopsis thaliana*. J Plant Res **113:** 139–148

Ben-Tov D, Abraham Y, Stav S, Thompson K, Loraine A, Elbaum R, de Souza A, Pauly M, Kieber JJ, Harpaz-Saad S (2015) COBRA-LIKE2, a member of the glycosylphosphatidylinositol-anchored COBRA-LIKE family, plays a role in cellulose deposition in Arabidopsis seed coat mucilage secretory cells. Plant Physiol **167:** 711–724

Blake AW, McCartney L, Flint JE, Bolam DN, Boraston AB, Gilbert HJ, Knox JP (2006) Understanding the biological rationale for the diversity of cellulose-directed carbohydrate-binding modules in prokaryotic enzymes. J Biol Chem **281:** 29321–29329

Blakeney AB, Harris PJ, Henry RJ, Stone BA (1983) A simple and rapid preparation of alditol acetates for monosaccharide analysis. Carbohydr Res **113:** 291–299

Caffall KH, Pattathil S, Phillips SE, Hahn MG, Mohnen D (2009) *Arabidopsis thaliana* T-DNA mutants implicate *GAUT* genes in the biosynthesis of pectin and xylan in cell walls and seed testa. Mol Plant **2:** 1000–1014

Dean GH, Zheng H, Tewari J, Huang J, Young DS, Hwang YT, Western TL, Carpita NC, McCann MC, Mansfield SD, et al (2007) The Arabidopsis *MUM2* gene encodes a β-galactosidase required for the production of seed coat mucilage with correct hydration properties. Plant Cell **19:** 4007–4021

Doyle JJ, Doyle JL (1990) Isolation of plant DNA from fresh tissues. Focus **12:** 13–15

Duan J, Zheng Y, Dong Q, Fang J (2004) Structural analysis of a pectic polysaccharide from the leaves of *Diospyros kaki*. Phytochemistry **65:** 609–615

Filisetti-Cozzi TMCC, Carpita NC (1991) Measurement of uronic acids without interference from neutral sugars. Anal Biochem **197:** 157–162

Gonzalez A, Mendenhall J, Huo Y, Lloyd A (2009) TTG1 complex MYBs, MYB5 and TT2, control outer seed coat differentiation. Dev Biol **325:** 412–421

Griffiths JS, Šola K, Kushwaha R, Lam P, Tateno M, Young R, Voiniciuc C, Dean G, Mansfield SD, DeBolt S, et al (2015) Unidirectional movement of cellulose synthase complexes in Arabidopsis seed coat epidermal cells deposit cellulose involved in mucilage extrusion, adherence, and ray formation. Plant Physiol **168:** 502–520

Griffiths JS, Tsai AY, Xue H, Voiniciuc C, Sola K, Seifert GJ, Mansfield SD, Haughn GW (2014) SALT-OVERLY SENSITIVE5 mediates Arabidopsis seed coat mucilage adherence and organization through pectins. Plant Physiol **165:** 991–1004

Guillon F, Tranquet O, Quillien L, Utille JP, Ordaz Ortiz JJ, Saulnier L (2004) Generation of polyclonal and monoclonal antibodies against arabinoxylans and their use for immunocytochemical location of arabinoxylans in cell walls of endosperm of wheat. J Cereal Sci **40:** 167–182

Harpaz-Saad S, McFarlane HE, Xu S, Divi UK, Forward B, Western TL, Kieber JJ (2011) Cellulose synthesis via the FEI2 RLK/SOS5 pathway and cellulose synthase 5 is required for the structure of seed coat mucilage in Arabidopsis. Plant J **68:** 941–953

Haughn GW, Western TL (2012) Arabidopsis seed coat mucilage is a specialized cell wall that can be used as a model for genetic analysis of plant cell wall structure and function. Front Plant Sci **3:** 64

Hayashi T, Marsden MP, Delmer DP (1987) Pea xyloglucan and cellulose. VI. Xyloglucan-cellulose interactions *in vitro* and *in vivo*. Plant Physiol **83:** 384–389

Huang J, DeBowles D, Esfandiari E, Dean G, Carpita NC, Haughn GW (2011) The Arabidopsis transcription factor LUH/MUM1 is required for extrusion of seed coat mucilage. Plant Physiol **156:** 491–502

Kabel MJ, van den Dorne H, Vincken JP, Voragen AGJ, Schols HA (2007) Structural differences of xylans affect their interaction with cellulose. Carbohydr Polym **69:** 94–105

Köhnke T, Östlund A, Brelid H (2011) Adsorption of arabinoxylan on cellulosic surfaces: influence of degree of substitution and substitution pattern on adsorption characteristics. Biomacromolecules **12:** 2633–2641

Kong Y, Zhou G, Abdeen AA, Schafhauser J, Richardson B, Atmodjo MA, Jung J, Wicker L, Mohnen D, Western T, et al (2013) GALACTURONOSYLTRANSFERASE-LIKE5 is involved in the production of Arabidopsis seed coat mucilage. Plant Physiol **163:** 1203–1217

Koornneef M (1981) The complex syndrome of *ttg* mutants. Arabidopsis Inf Serv **18:** 45–51

Langmuir I (1918) The adsoprtion of gases on plane surfaces of glass, mica and platinum. J Am Chem Soc **40:** 1361–1403

Le BH, Cheng C, Bui AQ, Wagmaister JA, Henry KF, Pelletier J, Kwong L, Belmonte M, Kirkbride R, Horvath S, et al (2010) Global analysis of gene activity during Arabidopsis seed development and identification of seed-specific transcription factors. Proc Natl Acad Sci USA **107:** 8063–8070

Lindberg B, Mosihuzzaman M, Nahar N, Abeysekera RM, Brown RG, Willison JHM (1990) An unusual (4-O-methyl-D-glucurono)-D-xylan isolated from the mucilage of seeds of the quince tree (Cydonia oblonga). Carbohydr Res **207:** 307–310

Lopez M, Bizot H, Chambat G, Marais MF, Zykwinska A, Ralet MC, Driguez H, Buléon A (2010) Enthalpic studies of xyloglucan-cellulose interactions. Biomacromolecules **11:** 1417–1428

Macquet A, Ralet MC, Kronenberger J, Marion-Poll A, North HM (2007a) In situ, chemical and macromolecular study of the composition of *Arabidopsis thaliana* seed coat mucilage. Plant Cell Physiol **48:** 984–999

Macquet A, Ralet MC, Loudet O, Kronenberger J, Mouille G, Marion-Poll A, North HM (2007b) A naturally occurring mutation in an *Arabidopsis* accession affects a β-D-galactosidase that increases the hydrophilic potential of rhamnogalacturonan I in seed mucilage. Plant Cell **19:** 3990–4006

Mazeau K, Charlier L (2012) The molecular basis of the adsorption of xylans on cellulose surface. Cellulose **19:** 337–349

Mendu V, Griffiths JS, Persson S, Stork J, Downie AB, Voiniciuc C, Haughn GW, DeBolt S (2011) Subfunctionalization of cellulose synthases in seed coat epidermal cells mediates secondary radial wall synthesis and mucilage attachment. Plant Physiol **157:** 441–453

Mohnen D (2008) Pectin structure and biosynthesis. Curr Opin Plant Biol **11:** 266–277

Mühlethaler K (1950) The structure of plant slimes. Exp Cell Res **1:** 341–350

Naran R, Chen G, Carpita NC (2008) Novel rhamnogalacturonan I and arabinoxylan polysaccharides of flax seed mucilage. Plant Physiol **148:** 132–141

North HM, Berger A, Saez-Aguayo S, Ralet MC (2014) Understanding polysaccharide production and properties using seed coat mutants: future perspectives for the exploitation of natural variants. Ann Bot (Lond) **114:** 1251–1263

Oka T, Nemoto T, Jigami Y (2007) Functional analysis of *Arabidopsis thaliana* RHM2/MUM4, a multidomain protein involved in UDP-D-glucose to UDP-L-rhamnose conversion. J Biol Chem **282:** 5389–5403

Penfield S, Meissner RC, Shoue DA, Carpita NC, Bevan MW (2001) MYB61 is required for mucilage deposition and extrusion in the *Arabidopsis* seed coat. Plant Cell **13:** 2777–2791

Podoly E, Hanin G, Soreq H (2010) Alanine-to-threonine substitutions and amyloid diseases: butyrylcholinesterase as a case study. Chem Biol Interact **187:** 64–71

Rautengarten C, Usadel B, Neumetzler L, Hartmann J, Büssis D, Altmann T (2008) A subtilisin-like serine protease essential for mucilage release from Arabidopsis seed coats. Plant J **54:** 466–480

Reis D, Vian B, Chanzy H, Roland JC (1991) Liquid crystal-type assembly of native cellulose-glucuronoxylans extracted from plant cell wall. Biol Cell **73:** 173–178

Rerie WG, Feldmann KA, Marks MD (1994) The GLABRA2 gene encodes a homeo domain protein required for normal trichome development in Arabidopsis. Genes Dev **8:** 1388–1399

Ridley BL, O'Neill MA, Mohnen D (2001) Pectins: structure, biosynthesis, and oligogalacturonide-related signaling. Phytochemistry **57:** 929–967

Saez-Aguayo S, Ralet MC, Berger A, Botran L, Ropartz D, Marion-Poll A, North HM (2013) PECTIN METHYLESTERASE INHIBITOR6 promotes *Arabidopsis* mucilage release by limiting methylesterification of homogalacturonan in seed coat epidermal cells. Plant Cell **25:** 308–323

Sullivan S, Ralet MC, Berger A, Diatloff E, Bischoff V, Gonneau M, Marion-Poll A, North HM (2011) CESA5 is required for the synthesis of cellulose with a role in structuring the adherent mucilage of Arabidopsis seeds. Plant Physiol **156:** 1725–1739

Tan L, Eberhard S, Pattathil S, Warder C, Glushka J, Yuan C, Hao Z, Zhu X, Avci U, Miller JS, et al (2013) An *Arabidopsis* cell wall proteoglycan consists of pectin and arabinoxylan covalently linked to an arabinogalactan protein. Plant Cell **25:** 270–287

Thibault JF (1979) Automatisation du dosage des substances pectiques par la méthode au métahydroxydiphényle. Lebensml Wiss Technol **12:** 247–251

Usadel B, Kuschinsky AM, Rosso MG, Eckermann N, Pauly M (2004) RHM2 is involved in mucilage pectin synthesis and is required for the development of the seed coat in Arabidopsis. Plant Physiol **134:** 286–295

Vincken JP, de Keizer A, Beldman G, Voragen AG (1995) Fractionation of xyloglucan fragments and their interaction with cellulose. Plant Physiol **108:** 1579–1585

Voiniciuc C, Günl M, Schmidt MHW, Usadel B (2015a) Highly branched xylan made by IRREGULAR XYLEM14 and MUCILAGE-RELATED21 links mucilage to Arabidopsis seeds. Plant Physiol **169:** 2481–2495

Voiniciuc C, Schmidt MHW, Berger A, Yang B, Ebert B, Scheller HV, North HM, Usadel B, Günl M (2015b) MUCILAGE-RELATED10 produces galactoglucomannan that maintains pectin and cellulose architecture in Arabidopsis seed mucilage. Plant Physiol **169:** 403–420

Voiniciuc C, Yang B, Schmidt MH, Günl M, Usadel B (2015c) Starting to gel: how Arabidopsis seed coat epidermal cells produce specialized secondary cell walls. Int J Mol Sci **16:** 3452–3473

Walker M, Tehseen M, Doblin MS, Pettolino FA, Wilson SM, Bacic A, Golz JF (2011) The transcriptional regulator LEUNIG_HOMOLOG regulates mucilage release from the Arabidopsis testa. Plant Physiol **156:** 46–60

Western TL (2006) Changing spaces: the *Arabidopsis* mucilage secretory cells as a novel system to dissect cell wall production in differentiating cells. Can J Bot **84:** 622–630

Western TL, Burn J, Tan WL, Skinner DJ, Martin-McCaffrey L, Moffatt BA, Haughn GW (2001) Isolation and characterization of mutants defective in seed coat mucilage secretory cell development in Arabidopsis. Plant Physiol **127:** 998–1011

Western TL, Skinner DJ, Haughn GW (2000) Differentiation of mucilage secretory cells of the Arabidopsis seed coat. Plant Physiol **122:** 345–356

Western TL, Young DS, Dean GH, Tan WL, Samuels AL, Haughn GW (2004) *MUCILAGE-MODIFIED4* encodes a putative pectin biosynthetic enzyme developmentally regulated by *APETALA2, TRANSPARENT TESTA GLABRA1*, and *GLABRA2* in the Arabidopsis seed coat. Plant Physiol **134:** 296–306

Willats WG, McCartney L, Knox JP (2001) In-situ analysis of pectic polysaccharides in seed mucilage and at the root surface of *Arabidopsis thaliana*. Planta **213:** 37–44

Windsor JB, Symonds VV, Mendenhall J, Lloyd AM (2000) Arabidopsis seed coat development: morphological differentiation of the outer integument. Plant J **22:** 483–493

Yanagisawa T, Kiribuchi-Otobe C, Yoshida H (2001) An alanine to threonine change in the Wx-D1 protein reduces GBSS I activity in waxy mutant wheat. Euphytica **121:** 209–214

Young RE, McFarlane HE, Hahn MG, Western TL, Haughn GW, Samuels AL (2008) Analysis of the Golgi apparatus in *Arabidopsis* seed coat cells during polarized secretion of pectin-rich mucilage. Plant Cell **20:** 1623–1638

Yu L, Shi D, Li J, Kong Y, Yu Y, Chai G, Hu R, Wang J, Hahn MG, Zhou G (2014) CELLULOSE SYNTHASE-LIKE A2, a glucomannan synthase, is involved in maintaining adherent mucilage structure in Arabidopsis seed. Plant Physiol **164:** 1842–1856

Zykwinska AW, Ralet MC, Garnier CD, Thibault JF (2005) Evidence for in vitro binding of pectin side chains to cellulose. Plant Physiol **139:** 397–407